

# Critical Grain Size of Fine Aggregates in the View of the Rheology of Mortar

Dongyeop Han<sup>1)</sup>, Jae Hong Kim<sup>2),\*</sup> , Jin Hyun Lee<sup>2)</sup>, and Su-Tae Kang<sup>3)</sup>

(Received August 28, 2016, Accepted September 6, 2017, Published online December 7, 2017)

**Abstract:** The aim of this research was to investigate the validity of the Krieger–Dougherty model as a quantitative model to predict the viscosity of mortar depending on various aggregate sizes. The Krieger–Dougherty model reportedly predicted the viscosity of a suspension, which includes cement-based materials. Concrete or mortar incorporates natural resources, such as sand and gravel, referred to as aggregates, which can make up as much as 80% of the mixture by volume. Cement paste is a suspending medium at fresh state and then becomes a binder to link the aggregate after its hydration. Both the viscosity of the suspending medium and the characteristics of the aggregates, therefore, control the viscosity of the cement-based materials. In this research, various sizes and gradations of fine aggregate samples were prepared. Workability and rheological properties were measured using fresh-state mortar samples and incorporating the various-sized fine aggregates. Yield stress and viscosity measurements were obtained by using a rheometer. Based on the packing density of each fine aggregate sample, the viscosity of the mortar was predicted with the Krieger–Dougherty model. In addition, further adjustments were made to determine the water absorption of fine aggregates and was transferred from successful experiment to simulation for more accurate prediction. It was also determined that both yield stress and viscosity increase when the fine aggregate mean size decreases throughout the mix. However, when the mean size of the fine aggregates is bigger than 0.7 mm, the yield stress is not affected by the size of the fine aggregate. Additionally, if aggregate grains get smaller up to 0.3 mm, their water absorption is critical to the rheological behavior.

**Keywords:** mortar, rheology, viscosity, fine aggregate, grain size, Krieger–Dougherty equation.

## 1. Introduction

Viscosity is defined as resistance to flow of fluid under shear stress and taken as the ratio between the shear stress and shear rate (George and Qureshi 2013). Viscosity helps prevent segregation during handling processes such as delivering, and placing for cementitious materials such as mortar or concrete (Khayat 1995). In a concrete mixture, the segregation of coarse aggregate is dominated by the viscosity of mortar. To achieve a high performance on its strength and durability, securing the viscosity for a stable mix becomes more important. On the other hand, an unstable supply of river sand and gravel due to the depletion of natural resources results in the use of various types of

coarse and fine aggregates, which include crushed, manufactured, recycled, or marine aggregates. Their physical properties including shape, size, texture, and grading including micro-fines can vary significantly from the reference state of aggregates that originated in a river. Even though they marginally satisfy the standard of aggregates, its poor quality causes difficulty in mix proportioning (Bairagi et al. 1990; Goltermann and Johansen 1997). Also the physical properties of the aggregate affect the performance of concrete and especially dominate workability in its fresh state (Erdoğan and Fowler 2005; Westerholm et al. 2008; Nanthagopalan and Santhanam 2011; Wallevik and Wallevik 2011; Quiroga and Fowler 2004; Mahmoodzadeh and Chidiac 2013). Therefore, evaluating the aggregate effect on the viscosity of freshly mixed cementitious materials allows us to control and guide the selection of the proper type of aggregates.

Based on the idea of coarse aggregates suspended in mortar, the viscosity of mortar dominates the segregation resistance and rheological behavior of the concrete mixture. Predicting viscosity of mortar, composed of fine aggregate and cement paste goes back to the principles behind aggregate particles suspended in cement paste (Erdem et al. 2010; Hidalgo et al. 2009; Toutou and Roussel 2006). This study analyzes the size effect of fine aggregates on the viscosity of the mortar. For this portion of the study we tested mono-sized sands with 10 different diameters, which were mixed

<sup>1)</sup>Department of Architectural Engineering, Engineering Research Institute, Gyeongsang National University, Jinju, South Korea.

<sup>2)</sup>School of Urban and Environmental Engineering, Ulsan National Institute of Science and Technology, Ulsan, South Korea.

\*Corresponding Author; E-mail: jaekim@unist.ac.kr

<sup>3)</sup>Department of Civil and Environmental Engineering, Daegu University, Gyeongsan, South Korea.

with a constant proportioning ratio. Blending the mono-sized sands required gap grading and controlled packing density of fine aggregates (Goltermann and Johansen 1997; Park et al. 2004). The second research objective focuses on the effect of packing density and the associated rheological properties of the mortar samples. The third objective is to determine the effect of aggregates size on their water absorption and the subsequent viscosity of mortar mixtures.

## 2. Materials and Sample Preparation

### 2.1 Mortar Samples

The fine aggregate used was natural river sand, which had various particle size distributions. A control sample was made up of natural river sand generally used for concrete mix proportioning. Table 1 reports the sieve test results obtained by ASTM C136 (ASTM International 2006), and the grading curve was within the recommendation range for concrete mix. The mean size and fineness modulus of the control sand sample were 0.71 mm and 2.39, respectively. The specific gravity was 2.60. The other samples were prepared by controlling the size of sand grains. Two sets of sieves were used for this experiment: (1) A set of sieves from ASTM C136 standard, reported in Table 1, and (2) a set of sieves for further detail analysis with opening sizes of 2.00 mm (No. 10), 0.85 mm (No. 20), 0.43 mm (No. 40), 0.25 mm (No. 60), and 0.15 mm (No. 100). The two sets of sieves handled 10 different size sand samples. The mono-size sand samples were prepared with retained sand on each sieve following the test for each set of sieves. For instance, using the ASTM C136 sieve set, the mean size of the sand sample retained on No. 16 sieve was calculated by averaging the opening sizes of the No. 8 sieve and No. 16 sieve, which determined a mean size of 1.77 mm and an error bound of  $\pm 0.59$  mm. The sand samples prepared with two sets of sieves are summarized in Table 2 with the samples' fundamental properties. G samples were composed mono-sized grains having a mean designated mean size. M 1.33, M 1.04 and M 0.66 samples were produced by mixing (1) G 1.77 and G 0.89; (2) G 1.77, G 0.89 and G 0.45; and (2) G 0.89 and G 0.45, respectively. They were mixed using a ratio of 1:1 or 1:1:1 by mass.

Depending on the gradation of sand samples, packing density varies, and a mixed sand sample is expected to have a higher packing density. The packing density is the main factor used to determine the viscosity in the Krieger–Dougherty model (Wildemuth and Williams 1984; Khodakov 2004). For mortar, under this research scope, in which the mortar is a suspension of fine aggregate to cement paste, the packing density of each dried sand sample was measured by following method:

1. Fill the fine aggregate sample in a 1-L steel cylinder and measure its weight. The fine aggregate sample should then be fully packed using a rubber hammer and the surface leveled.
2. Calculate the volume of the fine aggregate sample by dividing the weight measured from the previous step by the density of the fine aggregates. The volume occupied by the fine aggregates, per unit volume, would be the packing density. Consequently, the maximum fillable volume ratio of fine aggregates can be obtained for each sample. The measured packing density value of each sample is summarized in Table 2.

The densest packing of uniform spheres is given by closed-packing microstructures. Face centered cubic (FCC) or hexagonal close packing (HCP) generates the highest packing density,  $\pi/3\sqrt{2} = 0.74$ . In contrast, Song et al. (2008) analytically determined that random close packing (irregular or jammed packing) does not exceed the value of 0.634. The experiment in this study corresponds to the case, and the margin of the spherical diameter in Table 2 addresses the excess of jammed packing. With a margin larger than  $\pm 0.2$  mm, G 1.77, G 1.43, G 0.89 and G 0.64 exceeded the maximum jammed packing. Thus, the mixed samples and the river sand certainly increased the packing beyond the limit.

The sieve test required oven-dried sand samples; however, when the sand sample is mixed with cement paste as a mortar, the oven-dried sand sample absorbs the mixing water. Hence, it was necessary to determine the absorption rate to calculate the saturated but surface dry (SSD) condition of each sample. Furthermore, since smaller sizes of fine aggregates have higher specific surface areas, fine aggregate samples with the smaller mean size absorbed more water than the larger fine aggregates. This relates to the solid

**Table 1** The result of sieve analysis of 1000 g sand sample.

Sieve no.	Sieve size (mm)	Percent passing (%)
4	4.75	100
8	2.36	97
16	1.18	90
30	0.6	56
50	0.3	16
100	0.15	2
Pan	–	–

**Table 2** Fundamental properties of the fine aggregate samples.

Sample	Mean size (mm)	Error bound (mm)	Packing density	Absorption ratio (%)
G 1.77	1.77	±0.59	0.645	2.32
G 1.43	1.43	±0.58	0.656	1.97
G 0.89	0.89	±0.29	0.644	1.93
G 0.64	0.64	±0.21	0.640	3.49
G 0.45	0.45	±0.15	0.633	3.50
G 0.34	0.34	±0.09	0.626	7.26
M 1.33	1.33	–	0.662	1.83
M 1.04	1.04	–	0.683	4.88
M 0.66	0.67	–	0.671	2.99
Sand	0.71	–	0.695	2.59

concentration of mortar and its need for a water-to-cement ratio. When this ratio is properly applied, it gives the mortar a higher yield stress and viscosity. The absorption ratio of each fine aggregate sample was evaluated based on ASTM C128 (ASTM International 2015). Table 2 lists the fine aggregate samples' absorption rates. The absorption ratio increased as the mean size of the fine aggregate sample decreased, as expected. Notably, for G 0.34, about 7.26% of the highest absorption was observed.

For all mortar mixtures, the mix proportion was manually selected to show a rheological behavior sensitive to the aggregate condition. The water-to-cement ratio and sand-to-cement ratio were fixed to 0.45 and 1.2, respectively. The volume fractions of water, cement, and sand were then 0.366, 0.259, and 0.375, respectively. Commercially available ordinary Portland cement was used, which is equivalent to the Type I cement of ASTM C150 (ASTM International 2012). According to the information provided by the manufacturer, the specific gravity of the cement was 3.14 and the Blaine value was 335 m<sup>2</sup>/kg. The chemical composition of the cement used is shown in Table 3. A high-range water-reducing admixture (HRWRA) was added to remove yield stress effect from mini slump flow and channel flow tests of the samples. The HRWRA dosage was 0.6% by cement mass, and was a polycarboxylate-based solution with a solid content of 22%. Additionally, to prevent excessive bleeding, 0.1% by cement weight of viscosity modifying admixture (VMA) was added. All used chemical admixtures are commercially available products in South Korea. For mortar mixing, a 5 L planetary mortar mixer was used. Figure 1 shows the mixing protocol. As the first step, all materials were placed in a mixing bowl and mixed at the first (low) speed for 2 min. When resting for 1 min and during this interval, the materials on side of the mixing bowl was scraped down by a scraper. For the final mixing, the

materials were mixed at the second speed for 2 min following discharge and prepared for testing within 4 min. Hence the mortar samples were tested 9 min after water contact with the cement.

### 3. Tests Results

#### 3.1 Workability of the Mortar Samples

To evaluate the workability of fresh state mortar depending on the sand size, mini-slump flow test and channel flow test were conducted. Basically, the mini-slump flow test was executed with the same method of ASTM C1611 (ASTM International 2010), but a smaller cone mold was used for the mortar consistency test. The dimension of the mini-slump cone is 70 mm-diameter at the top and 100 mm-diameter at the bottom with a height of 50 mm. The channel flow test measure the one-sided flow of a cube sample having 100 mm on each side (Kim et al. 2014, 2015, 2017). For both tests, the measured data was (1) flowing distance and (2) the time duration until flowing stopped.

Table 4 reports the results of the mini-slump flow and the channel flow methods, where the fine aggregate size effects on the mortar workability is found. Generally, as the mean size of fine aggregate decreased, both final flow distance and stoppage time duration also decreased. This trend was confirmed within a lower range of 0.89 mm (the mean particle size of G 0.89), and no clear trend was observed with coarser particles. For mixed fine aggregate samples, the undisturbed workability was also found on the M 1.33 and M 1.04 samples which have a bigger mean size of fine aggregate than G 0.89. Meanwhile, M 0.66 achieved a smaller mean size, a higher mini-slump flow and a longer stoppage time, as expected. Therefore, it is concluded that because the fine aggregates consist of smaller particles, the fluidity is

**Table 3** Chemical composition of ordinary Portland cement.

Oxide	CaO	SiO <sub>2</sub>	Al <sub>2</sub> O <sub>3</sub>	Fe <sub>2</sub> O <sub>3</sub>	MgO	SO <sub>3</sub>	K <sub>2</sub> O	Na <sub>2</sub> O	TiO <sub>2</sub>
Content (%)	65.47	17.71	4.50	3.37	3.29	3.44	1.11	0.16	0.31

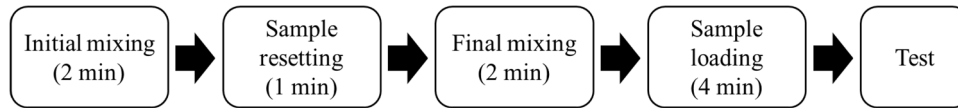


Fig. 1 Mixing protocol for mortar mixing.

Table 4 Workability tests results.

Sample	Mini-slump flow		Channel flow	
	Flow (mm)	T <sub>f</sub> (s)	Flow (mm)	T <sub>f</sub> (s)
G 1.77	280	30	830	70
G 1.43	280	27	740	96
G 0.89	270	23	630	70
G 0.64	240	22	680	88
G 0.45	230	13	500	90
G 0.34	120	8	310	30
M 1.33	290	60	690	110
M 1.04	270	60	620	80
M 0.66	290	60	700	120
Sand	260	26	750	78

decreased, so viscosity (defined as the invert of fluidity in rheology) increased. Note that no matter what the mean size of the fine aggregates, the well-graded fine aggregates can have a good fluidity and a high resistance to aggregate segregation. Additionally, the fine aggregate samples composed of a bigger mean size (1.43 mm or mean particle size of G 1.43), are susceptible to segregation due to their homogeneous grading even though they had a higher mini-slump flow indicating good workability.

### 3.2 Rheology of the Mortar Samples

To measure the rheological properties of the mortar samples, their flow curves were measured using a commercial rheometer from Thermo Scientific Inc. with a building materials cell (BMC) unit. Generally, a rotational viscometer (or rheometer) measures torque during rotation of a coaxial cylinder rotor. In the case of mortar, however, a larger size of fine aggregate causes a slip on the surface of the cylinder rotor and the inner wall of the outer cylinder (cup), which sometimes results in plug flow around the rotor. The BMC used in this study had a vane rotor and slits on the inner wall to prevent slip and plug flow. Figure 2 shows the structure and dimension of rotational viscometer. The inner diameter of the cylinder was 74 mm, and the rotating diameter of the vane was 50 mm. The sample was filled to about 130 mm in height and the torque was measured at programmed rotational speeds. The programmed rotational speed protocol is as follows: The rotational speed was increased by 0.8 rotation per second (rps) increments until it reached 8.0 rps. Each rotational speed stage was maintained for five seconds. After reaching 8.0 rps, the rotational speed was decreased by 0.8 rps increments until 0 rps. From these step-up and step-down protocols, two flow curves (up curve, and down curve)

were obtained (Ferron et al. 2007). In this study scope, there was no difference between up and down curves, which means there was no thixotropy within 2 min of the measuring period cessation.

The BMC used in this research had a wide-gap cylindrical geometry; thus, a linear shear rate on the radial direction could not be applied on the measured samples. Furthermore, a Bingham fluid like the mortar samples in the zero-shearing zone can occur near the wall of the cylinder. In this case, the Reiner–Riwlin equation (Koehler and Fowler 2004) separately considers whether the sample in the viscometer flowed for the entire range or the sample in the viscometer only partially flowed. When a Bingham fluid flows for the entire range, the relation between torque and rotational speed is expressed as follows:

$$\Omega = \frac{T}{8\pi^2 h \mu_p} \left( \frac{1}{R_1^2} - \frac{1}{R_2^2} \right) - \frac{\tau_y}{2\pi \mu_p} \ln \left( \frac{R_2}{R_1} \right) \quad (1)$$

where  $\Omega$  is the rotational speed (rps),  $T$  is the torque measured (N m),  $h$  is the height of the vane,  $R_1$  is the radius of the vane, and  $R_2$  is the inner radius of the cylinder. The yield stress and plastic viscosity of the Bingham fluid model is then obtained from the slope and x-intercept of Eq. (1). The existence of dead zone (no shear flow) near the inner wall of the container changes the relationship as follows:

$$\Omega = \frac{T}{8\pi^2 h \mu_p} \left( \frac{1}{R_1^2} - \frac{2\pi h \tau_y}{T} \right) - \frac{\tau_y}{4\pi \mu_p} \ln \left( \frac{T}{2\pi h \tau_y R_1^2} \right) \quad (2)$$

Under these conditions, the yield stress and the plastic viscosity cannot be calculated unless the measured data points are fitted using a nonlinear optimization method.

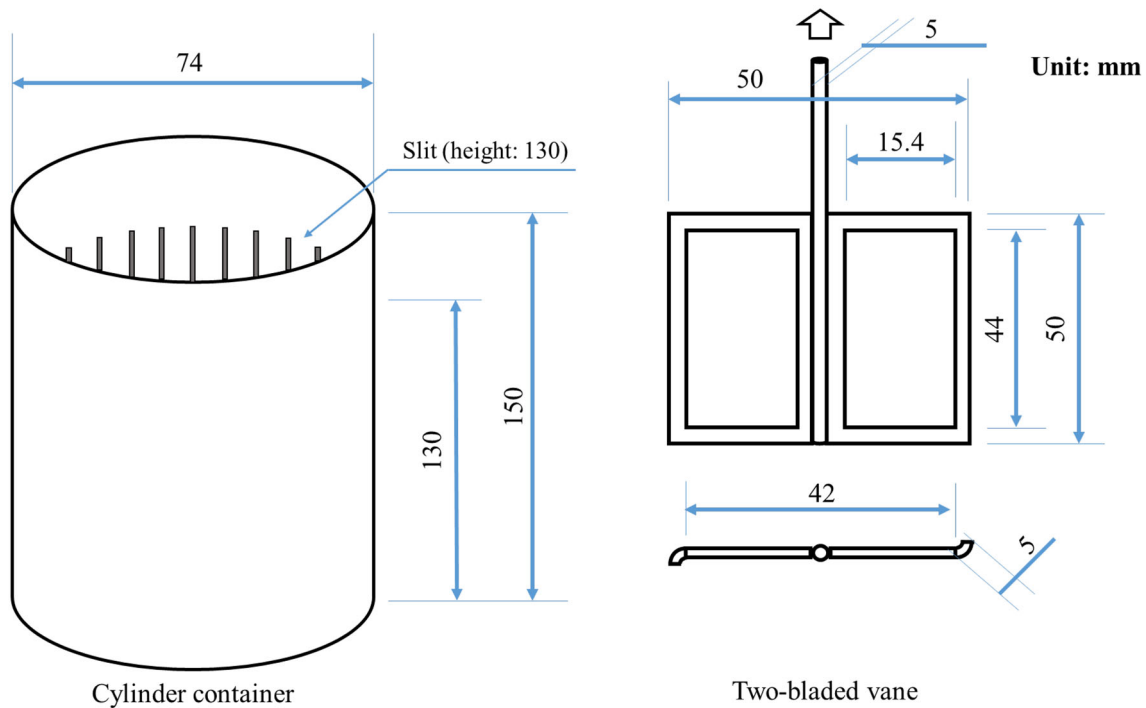


Fig. 2 Dimension of the BMC cylinder container and vane.

Figure 3 shows the flow curves of four representative samples. In the graph, the points are the rheological measurements at each rotational speed, and the dashed lines show the applicable results of the Reiner–Riwlin equation for the case of partial shear flow. The rheological parameters of yield stress and viscosity, evaluated by Eqs. (1) and (2) are compared in Fig. 4. Assuming shear flow occurred during entire range of the sample, Eq. (1) gave a slightly lower yield stress and higher viscosity values than those given by Eq. (2), which calculated a partial shear flow in the sample. Further, the difference between two evaluations increased when a sample had a higher yield stress. The difference caused by the partial shear flow was maximized with G 0.34 showing the highest yield stress. Here, the shear flow range is considered within 29 mm of the center radius compared with the 37 mm inner radius of the container ( $29/37 = 78\%$  in radius). The rotational radius was calculated

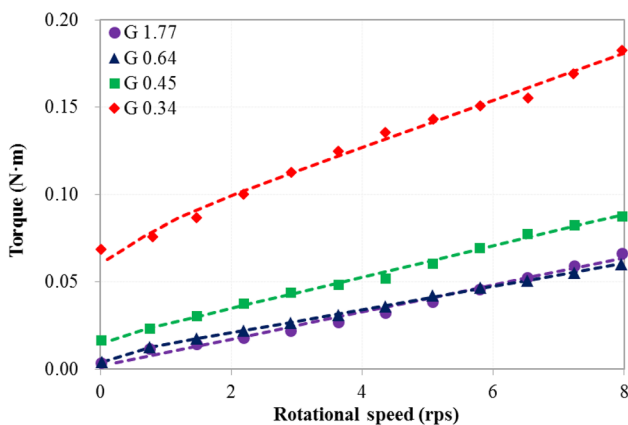


Fig. 3 Flow curve measurement.

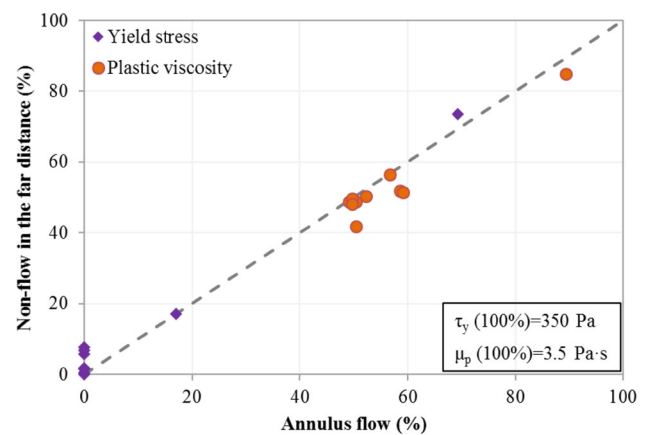


Fig. 4 Yield stress and plastic viscosity according to the flow assumption.

by  $R_2 = \sqrt{T/2\pi h\tau_y}$  at 0.8 rps (0.064 N m). The other mortar samples had an effective radius within a range of less than 85% of the inner diameter of the container, where the differences of the two model equations are negligible. Therefore, Eq. (2) was applied to evaluate the rheological parameters of the G 0.34 sample only. To further analyze the mortar samples, the rheological properties of the base cement paste (interstitial fluid for the mortar suspensions) were additionally measured. The sample adopts the same mix proportion as the mortar samples, but fine aggregates were excluded ( $w/cm = 0.45$ , HRWRA = 0.6% and VMA = 0.1%). As a result, the base cement paste sample showed a low viscosity compared to the mortar samples and a negligible yield stress. Applying a Newtonian fluid model evaluated its viscosity at 0.37 Pa·s.

## 4. Discussion

Figure 5 shows the influence of fine aggregate size on the yield stress and plastic viscosity of the mortar samples. The round points show the G sample data to be consistent with approximately mono-sized sand, and the triangle points show the M sample data. Regardless of the grading characteristic, the plastic viscosity gradually increases with the smaller mean size of the fine aggregates. The trend, however, disappears when the mean size exceeds 0.7 mm. All mortar samples showed zero yield stress and 1.7 Pa·s viscosity when the mean size of the fine aggregates was larger than 0.7 mm. The trend for the yield stress was also similar. That shows the tendency of a mortar sample incorporating fine aggregates bigger than a certain size to show rheological properties independent of its grading characteristics. The effect of fine aggregates on the resultant rheological behavior is controlled only by its content in mix proportion, which is also related to the workability test (Sect. 3.1) results: No influence of mean size was found on the mini-slump flow when the sample mean size was bigger than 0.89 mm (see samples G 1.77, G 1.43 and G 0.89).

The Krieger–Dougherty model (Krieger and Dougherty 1959; Roussel et al. 2010) predicts the viscosity of the suspension using solid volume fraction, packing density and the intrinsic viscosity of particles:

$$\eta = \eta_s \left( 1 + \frac{\phi}{\phi_m} \right)^{-[\eta]\phi_m} \quad (3)$$

where  $\eta$  is the viscosity of suspension,  $\eta_s$  is the viscosity of the interstitial fluid,  $\phi$  is the volume fraction of the particles,  $\phi_m$  is the packing density, and  $[\eta]$  is the intrinsic viscosity. This model obviously shows the increased viscosity with increased solid volume fraction (Wildemuth and Williams 1984). In this research, the solid volume fraction of the mortar samples is applied at 0.4. The volume fraction of fine aggregates and the packing density of fine aggregates were measured as previously described. The intrinsic viscosity of  $[\eta]$  in Eq. (1) was 2.5 assuming the shape of individual fine aggregate particles as non-colloidal spheres. Table 5 calculates the viscosity values of mortar and the differences between calculated value and measured value based on the

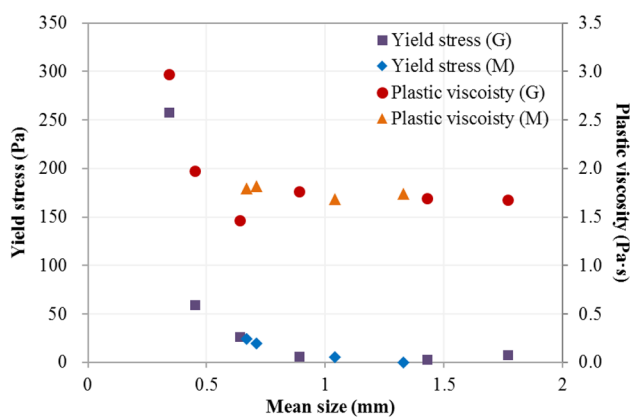


Fig. 5 Effect of mean size of the fine aggregate.

cement paste viscosity where  $\eta_0 = 0.37$  Pa·s described in Sect. 3.2.

The difference is within 10% excluding samples G 0.64 and G 0.34. Still it is needed to discuss the high error of G 0.64. It should be noted that its measured viscosity is out of trend, which strongly points to measurement error. Sample G 0.34 showed extremely high viscosity, which caused the estimation to lose its accuracy. Water absorption of fines reportedly maximizes with smaller particles, which will be discussed in the next paragraph. The other samples can be explained by the Krieger–Dougherty equation, which is also valid for the mixed sample case. Measurement of wet packing, contrary to the dry packing adopted in this study, is expected to decrease the difference because the hydrodynamic properties of grains are not consistent when they are floating in a suspended medium (Kwan et al. 2012). Additionally, as a possible factor, the chemical admixtures used in this research are affected by changing packing density under wet conditions, which induces errors between predicted viscosity and dry packing density. For better prediction, although the wet packing conditions of suspension should be evaluated with the influence of chemical admixtures, as per Bentz et al. (2012), it is difficult to evaluate the influence of superplasticizers on packing conditions of suspensions. Furthermore, according to Wallevik and Wallevik (2011), superplasticizer is considered to only affect yield stress of cement paste; furthermore, VMA changes the medium of the suspension rather than the particles. Although this theoretical background as per Quiroga and Fowler (2004) and Bentz et al. (2012) may not follow a prescribed methodology in a practical aspect, this research agrees with their findings that the addition of chemical admixtures to the samples can be considered a factor causing prediction error.

The viscosity estimation error for G 0.34 was approximately 63% in Table 5, and the sample gave the highest water absorption—more than double that of the other samples—as reported in Table 2. The following experiment was designed to verify that the water absorption generates error of the viscosity estimation. Two samples, G 0.45 and G 0.34, were compared. The difference in their water absorption was 3.50%, but their packing densities were very similar, 0.633 and 0.626, respectively. Simply adding 3.50% absorbed water to the S60 sample allows it to maintain same solid volume fraction as G 0.45. After the absorption rate was corrected for G 0.34, the value in parentheses, the rheology parameters and difference to the predicted values were added in Table 5. The prediction of rheological properties was possible at 0.34 mm of the fine aggregate sample size, while the workability difference was observed as smaller than 0.89 mm of the fine aggregate sample size. Therefore, it can be concluded that workability decreases with decreasing particle mean size and is only influenced by water absorption in a range from 0.34 to 0.89 mm. Considering the water absorption effect keeps the Krieger–Dougherty model valid, the hydrodynamic state of the mortar samples is consistent in the range of aggregate size.

The effect of the aggregates size, excluding the effect of their water absorption, can be analyzed based on a loosening

**Table 5** Comparing predicted viscosity value and measured viscosity value.

Sample	Predicted viscosity (Pa·s)	Measured viscosity (Pa·s)	Relative error for the prediction (%)
G 1.77	1.76	1.76	-0.02
G 1.43	1.73	1.72	-0.78
G 0.89	1.77	1.83	3.56
G 0.64	1.78	1.47	-17.54
G 0.45	1.80	1.98	9.83
G 0.34	1.82	2.971 (1.81)	63.04 (2.61)
M 1.33	1.72	1.74	1.42
M 1.04	1.67	1.69	1.33
M 0.66	1.69	1.80	6.22
Sand	1.64	1.82	10.87

phenomenon on the packing state. Cement paste, the interstitial fluid for the mortar samples, is not a liquid matter but another suspension at a micro-scale. The maximum particle size of Portland cement is less than 75 μm in a dry state, and its remained the same on a 45 μm-sieve making it practically less than 10% by mass. The cement particles place in between the aggregate particles results in the loosening effect on the packing of aggregates; hence, the packing density decreases. Applying the compressive packing model proposed by de Larrard and Sedran (2002) allows us to consider the loosening effect, and consequent packing density for  $d_1$ -dominant packing, which is calculated as

$$\phi_m = \frac{\beta_1}{1 - y_2 \left(1 - a_{12} \frac{\beta_1}{\beta_2}\right) - y_3 \left(1 - a_{13} \frac{\beta_1}{\beta_3}\right) - y_4 \left(1 - a_{14} \frac{\beta_1}{\beta_4}\right) - \dots} \quad (4)$$

where the loosening coefficient of  $a_{ij} = \sqrt{(1 - (1 - d_j/d_i)^{1.02})}$ . The parameters  $\beta_1, \beta_2, \beta_3, \dots$  are the packing density of each class of particles having the diameter of  $d_1, d_2, d_3, \dots$ , respectively, and their mutual volume fractions are given by  $y_1, y_2, y_3, \dots$ , respectively. Note that the mutual volume fractions were defined the volume fraction of each-class particles divided by the total volume fraction of all particles.

The mono-sized sand first takes the largest class of particles,  $d_1$ , and then the following classes of  $d_2, d_3, \dots$ , are reserved for cement particles classified in its dimension. Their packing densities can be assumed as constant,  $\beta_i = 0.634$  (theoretical value for random packing), because the packing density of mono-sized sand with a mean size of less than 1 mm, from G 0.89 to G 0.34 in this study, was within  $\pm 1.5\%$  error. Thus, the  $\beta$ -ratio in the denominator cancels out with the value of 1. In addition, only the packing of sand is investigated here; then, getting rid of the packing effect of cement particles gives

$$\phi_m = \frac{\beta_1}{1 + y_2 a_{12} + y_3 a_{13} + y_4 a_{14} + \dots} \cong \beta_1 (1 - y_2 a_{12} - y_3 a_{13} - y_4 a_{14} - \dots) \quad (5)$$

which is finally approximated by the binominal expansion. The loosening effect from the  $d_i$ -sized cement particle is  $y_i a_{1i} \times 100\%$  decrease in the packing density of sand. If  $d_2$ -sized particles take the remaining cement amount on the 45 μm-sieve, which is 4% of the total cement mass as an example, the volume fraction of  $d_2$ -sized particles is 0.0104 from that of the total cement amount (0.259). The value of  $y_2$  is then given by  $0.0104 / (0.0104 + 0.375) = 0.0398$  with the volume fraction of sand (0.375). The coefficient becomes  $a_{12} = \sqrt{(1 - (1 - 0.132)^{1.02})} = 0.367$  with  $d_2/d_1 = 0.045/0.34 = 0.132$ . Finally, the loosening effect of cement particles larger than 45 μm decreases 1.46% of the packing density. The decrease is within the range of fluctuation when the packing density of sand was measured. Therefore, the mortar sample incorporating the smallest sand particles (0.34 mm) was possibly predicted with the Krieger–Dougherty equation. If fine sand having the size of 0.1 mm is used, the loosening effect doubles and the original Krieger–Dougherty equation would lose its predicting accuracy. The loosening effect is expected to be maximized if a mix (1) incorporates finer sand or (2) uses coarser cement, showing a lower percentage passing on a 45 μm-

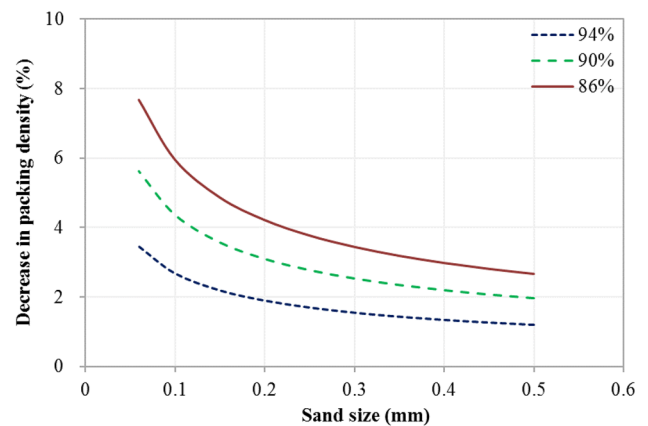


**Fig. 6** Decrease in packing density depending on the sand size.

sieve. Figure 6 shows the result of the parametric study calculating the loosening effect, where three plots assumes the passing percentage on a 45 µm-sieve by 94, 90 or 86%.

## 5. Conclusions

In this research, the rheological properties of fresh state mortar were evaluated depending on various mean sizes of fine aggregate, and the rheological properties were predicted using the Krieger–Dougherty model. This paper’s research experiment results can be summarized as follows;

1. Mini-slump and channel flow of mortar showed decreased flowing distance and reaching time with smaller fine aggregate grains. The workability change according to the dimension of aggregates can be related to the relationship between viscosity and the mean size of the fine aggregate sample.
2. The relation of torque-rotational speed can be analyzed with the Reiner–Rivlin model for quantitative expression of yield stress and viscosity of fresh-state mortar. From the analysis, as the mean size of the fine aggregate decreased, yield stress and viscosity of the fresh state mortar increased. However, the size of the fine aggregate did not influence the yield stress when the aggregate size exceeded 0.70 mm.
3. The Krieger–Dougherty model allows prediction of the viscosity of mortar, and the viscosity of mortar can be decreased with low packing density of fine aggregate. The packing density was increased from single-sized gradation to multi-sized gradation because of filling effect of various size particles.
4. Smaller grains of fine aggregates showed higher adsorption per unit mass. For air-dried conditions, since the mortar including the fine aggregate with higher absorption rate decreases water-to-cement ratio, yield stress and viscosity of the mortar can be increased. From the absorption rate measurement, when the mean size of the fine aggregate sample is higher than 0.34 mm (S60), the absorption rate of the fine aggregate is remarkably increased as the mean size of the fine aggregate is increased. In this case, compensating the absorption ratio provided a more accurate prediction of viscosity with the Krieger–Dougherty model.
5. Therefore, by using the method suggested in this research, the viscosity of a given mortar can be predicted by measuring the viscosity of cement paste and packing density of fine aggregate. This indicates that accurate prediction of the rheological behavior of mortar is possible by conducting a packing density test of various fine aggregate types.

## Acknowledgements

This research was supported by Basic Science Research Program through the National Research Foundation of

Korea (NRF) funded by the Ministry of Science, ICT and Future Planning (NRF-2015R1A1A1A05001382).

## Open Access

This article is distributed under the terms of the Creative Commons Attribution 4.0 International License (<http://creativecommons.org/licenses/by/4.0/>), which permits unrestricted use, distribution, and reproduction in any medium, provided you give appropriate credit to the original author(s) and the source, provide a link to the Creative Commons license, and indicate if changes were made.

## References

- ASTM International. (2006). *ASTM C136, standard test method for sieve analysis of fine and coarse aggregate*. West Conshohocken, PA: ASTM International. doi:10.1520/C0136.
- ASTM International. (2010). *ASTM C1611, standard test method for slump flow of self-consolidating concrete*. West Conshohocken: ASTM International.
- ASTM International. (2012). *ASTM C150, standard specification for Portland cement*. West Conshohocken: ASTM International.
- ASTM International. (2015). *ASTM C128, standard test method for density, relative density (specific gravity) and absorption of fine aggregate*. West Conshohocken, PA: ASTM International. doi:10.1520/C0128-15.2.
- Bairagi, N., Vidyadhara, H., & Ravande, K. (1990). Mix design procedure for recycled aggregate concrete. *Construction and Building Materials*, 4, 188–193.
- Bentz, D. P., Ferraris, C. F., Galler, M. A., Hansen, A. S., & Guynn, J. M. (2012). Influence of particle size distributions on yield stress and viscosity of cement–fly ash pastes. *Cement and Concrete Research*, 42, 404–409. doi:10.1016/j.cemconres.2011.11.006.
- de Larrard, F., & Sedran, T. (2002). Mixture-proportioning of high-performance concrete. *Cement and Concrete Research*, 32, 1699–1704. doi:10.1016/S0008-8846(02)00861-X.
- Erdem, K., Khayat, K. H., & Yahia, A. (2010). Correlating rheology of self-consolidating concrete to corresponding concrete-equivalent mortar. *ACI Materials Journal*, 106, 154–160.
- Erdoğan, S., & Fowler, D. (2005). Determination of aggregate shape properties using X-ray tomographic methods and the effect of shape on concrete rheology (No. ICAR 106-1), Austin, TX.
- Ferron, R., Gregori, A., Sun, Z., & Shah, S. (2007). Rheological method to evaluate structural buildup in self-consolidating concrete cement pastes. *ACI Materials Journal*, 104, 242–250.
- George, H., & Qureshi, F. (2013). *Newton’s law of viscosity*. Newtonian and non-Newtonian fluids: Encyclopedia Tri-bology. doi:10.1007/978-0-387-92897-5\_143.

- Goltermann, P., & Johansen, V. (1997). Packing of aggregates: an alternative tool to determine the optimal aggregate mix. *ACI Materials Journal*, *94*, 435–443.
- Hidalgo, J., Chen, C., & Struble, L. J. (2009). Correlation between paste and concrete flow behavior. *ACI Materials Journal*, *106*, 281–288.
- Khayat, K. (1995). Effects of antiwashout admixtures on fresh concrete properties. *ACI Materials Journal*, *92*, 164–171.
- Khodakov, G. (2004). On suspension rheology. *Theoretical Foundations of Chemical Engineering*, *38*, 400–439.
- Kim, J. H., Jang, H. R., & Yim, H. J. (2015). Sensitivity and accuracy for rheological simulation of cement-based materials. *Computers and Concrete*, *15*, 903–919. doi:10.12989/cac.2015.15.6.903.
- Kim, J. H., Lee, J. H., Shin, T. Y., & Yoon, J. Y. (2017). Rheological method for alpha test evaluation of developing superplasticizers' performance: Channel flow test. *Advances in Materials Science and Engineering*. doi:10.1155/2017/4214086.
- Kim, J., Yim, H., & Kwon, S. (2014). Quantitative measurement of the external and internal bleeding of conventional concrete and SCC. *Cement and Concrete Composites*, *54*, 34–39.
- Koehler, E., & Fowler, D. (2004). Development of a Portable rheometer for fresh Portland cement concrete (No. ICAR 105-3F), Austin, TX.
- Krieger, I. M., & Dougherty, T. J. (1959). A mechanism for non-newtonian flow in suspensions of rigid spheres. *Transactions Society of Rheology*, *3*, 137–152. doi:10.1122/1.548848.
- Kwan, A. K. H., Li, L. G., & Fung, W. W. S. (2012). Wet packing of blended fine and coarse aggregate. *Materials and Structures*, *45*, 817–828.
- Mahmoodzadeh, F., & Chidiac, S. (2013). Rheological models for predicting plastic viscosity and yield stress of fresh concrete. *Cement and Concrete Research*, *49*, 1–9.
- Nanthagopalan, P., & Santhanam, M. (2011). Fresh and hardened properties of self-compacting concrete produced with manufactured sand. *Cement and Concrete Composites*, *33*, 353–358.
- Park, T., Noh, M., & Park, C. (2004). Characterization of rheology on the multi-ingredients paste systems mixed with mineral admixtures. *Journal of the Korea Concrete Institute*, *16*, 241–248.
- Quiroga, P., & Fowler, D. (2004). The effects of aggregates characteristics on the performance of Portland cement concrete (No. ICAR 104-1F), Austin, TX.
- Roussel, N., Lemaitre, A., Flatt, R., & Coussot, P. (2010). Steady state flow of cement suspensions: A micromechanical state of the art. *Cement and Concrete Research*, *40*, 77–84.
- Song, C., Wang, P., & Makse, H. A. (2008). A phase diagram for jammed matter. *Nature*, *453*, 629–632. doi:10.1038/nature06981.
- Toutou, Z., & Roussel, N. (2006). Multi scale experimental study of concrete rheology: from water scale to gravel scale. *Materials and Structures*, *39*, 189–199. doi:10.1617/s11527-005-9047-y.
- Wallevik, O. H., & Wallevik, J. E. (2011). Rheology as a tool in concrete science: The use of rheographs and workability boxes. *Cement and Concrete Research*, *41*, 1279–1288. doi:10.1016/j.cemconres.2011.01.009.
- Westerholm, M., Lagerblad, B., Silfwerbrand, J., & Forssberg, E. (2008). Influence of fine aggregate characteristics on the rheological properties of mortars. *Cement and Concrete Composites*, *30*, 274–282.
- Wildemuth, C. R., & Williams, M. C. (1984). Viscosity of suspensions modeled with a shear-dependent maximum packing fraction. *Rheologica Acta*, *23*, 627–635. doi:10.1007/BF01438803.